Models of fluidized granular materials: examples of non-equilibrium stationary states

2005 J. Phys.: Condens. Matter 17 S2715

(http://iopscience.iop.org/0953-8984/17/24/022)

INSTITUTE OF PHYSICS PUBLISHING JOURNAL OF PHYSICS: CONDENSED MATTER

J. Phys.: Condens. Matter **17** (2005) S2715–S2730 doi:10.1088/0953-8984/17/24/022

Models of fluidized granular materials: examples of non-equilibrium stationary states

Andrea Puglisi[1], **Fabio Cecconi**[2] **and Angelo Vulpiani**[3]

[1] Laboratoire de Physique Theorique Batiment 210, Universitè de Paris-Sud, 91405 Orsay Cedex, France
[2] INFM Center for Statistical Mechanics and Complexity and Dipartimento di Fisica, Università 'La Sapienza', Piazzale A Moro 2, I-00185 Rome, Italy
[3] Dipartimento di Fisica, Università 'La Sapienza', INFM Center for Statistical Mechanics and Complexity (SMC), INFN Sezione di Roma-1 'La Sapienza', Piazzale A Moro 2, I-00185, Rome, Italy

Received 16 March 2005
Published 3 June 2005
Online at stacks.iop.org/JPhysCM/17/S2715

Abstract

We review some models of granular materials fluidized by means of external forces, such as random homogeneous forcing with damping, vibrating plates, flow in an inclined channel and flow in a double well potential. All these systems show the presence of density correlations and non-Gaussian velocity distributions. These models are useful in understanding the role of a kinetically defined 'temperature' (in this case the so-called *granular temperature*) in a non-equilibrium stationary state. In the homogeneously randomly driven gas the granular temperature is *different* from that of the driving bath. Moreover, two different granular materials mixed together may stay in a stationary state with different temperatures. At the same time, the granular temperature determines (as in equilibrium systems) the escape time in a double well potential.

1. Introduction

Granular materials such as sand, grains and powders exhibit a variety of remarkable behaviours which, in the last decades, have been extensively studied through a number of experiments, computer simulations and analytical techniques [1–3]. This paper aims to review the conceptual and technical difficulties encountered when the same statistical approach successfully applied to simple fluids is generalized and extended to study granular systems. The question whether the dynamics of a collection of inelastic particles is amenable to a hydrodynamical and even 'thermodynamical' description is a long-standing and still controversial issue of the general theory of granular matter.

In 1995, Du *et al* [4] proposed and studied a minimal model of a one-dimensional granular gas where N hard rods, constrained to move on the segment $[0, L]$, interact by instantaneous binary inelastic collisions with a restitution coefficient $r < 1$. A thermal wall of temperature T_b,

at the boundary $x = 0$, prevents the system from the cooling caused by inelasticity. When the leftmost particle bounces against the wall, it is reflected with a velocity drawn from a Gaussian distribution with variance T_b, and transfers the energy to the rest of the system. The main finding of the authors was that even at very small dissipation $1-r \sim 0$, hydrodynamic equations failed to reproduce the essential features of simulations. Simulations, indeed, showed that the system sets into an 'extraordinary' state with most of the particles moving slowly and very near the right wall, while most of the kinetic energy is concentrated in the leftmost particle. Reducing the dissipativity $1 - r$ at fixed N, the cluster near the wall becomes smaller and smaller. The authors also pointed out that a qualitative explanation of this clustering phenomenon could be found in the Boltzmann equation in the limit $N \to \infty$, $r \to 1$ with $N(1 - r) \sim 1$. We have reproduced the results of Du *et al* and found that the breakdown of the hydrodynamic approach can be ascribed to the peculiarities of the model.

First, the one-dimensional character generally represents an obstacle to the development of the hydrodynamic theory even for elastic systems, since transport coefficients usually diverge with system size at low dimension. Of course exceptions exist as shown in [5], where, under some particular circumstances, the hydrodynamics of a 1D inelastic system has been worked out.

Second, this model lacks a proper thermodynamic limit because when $N, L \to \infty$ (with $N/L =$ constant), both the mean kinetic energy and the mean dissipated power reduce to zero. This is consistent with the scenario suggested by the authors in which energy equipartition is broken and the description of the system in terms of macroscopic smooth quantities no longer holds. The proposed mechanism of energy injection may become strongly inefficient because, even at moderate inelasticities, it may involve only a few particles near the thermal wall. In this condition, thermodynamic observables such as mean kinetic energy or mean dissipated power are non-extensive quantities.

Third, the system has no proper elastic limit; indeed, when the dissipation is removed by setting $r \to 1$, the kinetic energy increases indefinitely due to the mechanical action of the wall that continuously injects energy into the system. The situations become even worse upon reducing the energy injection to zero to take the elastic limit: elastic collisions simply exchange velocities and the initial velocity distribution does not evolve at all.

In the following, we present and study a class of models where the aforementioned 'pathologies' are partly removed. The common feature of these models is the presence of a stochastic external driving which, acting statistically on each particle, destroys the anomalous configurations observed in [4]. Furthermore, the action of a damping term guarantees the existence of a smooth elastic limit. We shall see that although such systems display a 'less pathologic' behaviour, the existence of a hydrodynamical interpretation is still critical and dubious because it is affected by general conceptual problems [6]. The same difficulties, on the other hand, are also encountered in the interpretation of experimental studies on forced granular systems. For instance, a well known experiment by Jaeger *et al* [7] considers a container full of sand shaken from the bottom plate. When the shaking is very rapid, observations indicate that a few-grain thick boundary layer forms near the floor. Particles inside this layer move very quickly with sudden changes in their dynamics. At the top of the container, in contrast, particles move ballistically, undergoing very few collisions in their trajectory (Knudsen regime). Both layers cannot be described by hydrodynamics because the assumption of smooth variation of the velocity field is not satisfied. The same happens in molecular gases; however, for granular systems such boundary layers are macroscopic, and this seriously affects the prediction capability of hydrodynamic theories. Furthermore, the lack of a neat scale separation between the mean free time and the vibration period makes any hydrodynamic approach practically meaningless. On the other hand, it is also intrinsically unable to describe the slow grain

dynamics at slow tapping rates. In this case, indeed, the system reaches a sort of mechanical equilibrium characterized by an almost complete absence of motion [8]. Such an equilibrium is reached at different densities which—as the tapping goes on—slowly change with 'history'-dependent evolutions. This memory effect cannot be captured by the set of partial differential equations concerning ordinary hydrodynamics.

The paper is organized as follows. In section 2, we describe a model of granular gas introduced to remove the 'pathologies' affecting previous models, such as the lack of a well defined thermodynamic or elastic limit. In sections 3 and 4, we discuss simulations on different models for driven granular gas with non-homogeneous energy sources. In section 5, we discuss the fundamental problem of scale separation which undermines the development of a general hydrodynamic theory for granular flows. After having summarized the main failures of thermodynamic and hydrodynamic approaches to granular systems, we present, in section 6, a numerical experiment where thermodynamic concepts positively apply. In section 7 we finally draw some conclusions.

2. Homogeneous driving by random forces

In [9, 10], some of us introduced a kinetic model to describe a granular gas kept in a stationary state under the effect of both a damping term and external stochastic forcing. This model aims to reproduce the experimental situations in which an inelastic system is forced by shearing, shaking, air fluidization, and so on. All these energy sources supply the system with an 'internal energy' able to randomize the relative particle velocities. They basically act as a temperature source [11, 12] which favours the onset of steady regimes, but which, at the same time, introduces a systematic (non-random) friction which can be modelled by an effective damping term in the particle dynamics.

The randomly driven granular gas defined in [9] consists of an assembly of N identical hard objects (spheres, discs or rods) of mass m and diameter σ. We shall set $m = 1$ and $k_B = 1$ (Boltzmann's constant) in the following and assume that the grains move in a box of volume $V = L^d$. The dynamics of the system is the outcome of three physical effects: friction with the surroundings, random accelerations due to external driving, and inelastic collisions among the grains. The first two ingredients are modelled in the shape of Kramers' equations between two consecutive collisions:

$$\frac{\mathrm{d}}{\mathrm{d}t}\mathbf{x}_i(t) = \mathbf{v}_i(t) \tag{1}$$

$$\frac{\mathrm{d}}{\mathrm{d}t}\mathbf{v}_i(t) = -\frac{\mathbf{v}_i(t)}{\tau_b} + \sqrt{\frac{2T_b}{\tau_b}}\boldsymbol{\eta}_i(t). \tag{2}$$

The parameters τ_b (decorrelation time) and T_b (temperature) characterize the properties of the external bath. The function $\boldsymbol{\eta}_i(t)$ is the standard white noise: $\langle \boldsymbol{\eta}_i(t) \rangle = 0$ and $\langle \eta_i^\alpha(t)\eta_j^\beta(t') \rangle = \delta(t - t')\delta_{ij}\delta_{\alpha\beta}$ $(\alpha, \beta = x, y, z)$. This choice guarantees that Einstein's relation [13] is fulfilled in the elastic or collisionless regime. The inelastic collisions, in contrast, are considered at the kinetic level, because an impact instantaneously transforms the velocities of the grains involved. When particles i and j collide, their velocities are instantaneously changed into new velocities according to the following collision rule:

$$\mathbf{v}_i' = \mathbf{v}_i - \frac{1+r}{2}((\mathbf{v}_i - \mathbf{v}_j)\cdot\hat{\mathbf{n}})\hat{\mathbf{n}} \tag{3}$$

$$\mathbf{v}_j' = \mathbf{v}_j + \frac{1+r}{2}((\mathbf{v}_i - \mathbf{v}_j)\cdot\hat{\mathbf{n}})\hat{\mathbf{n}} \tag{4}$$

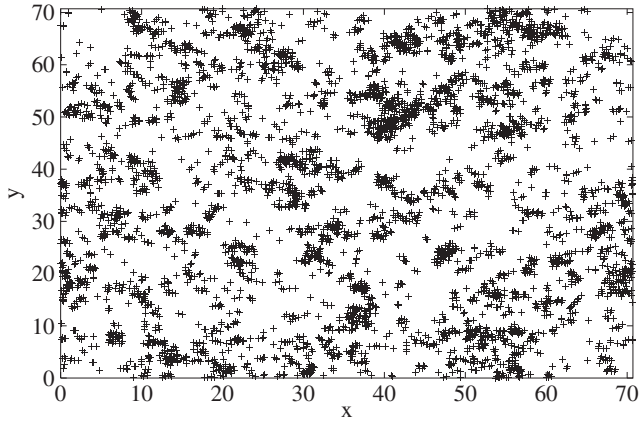

Figure 1. Density snapshots in the homogeneously driven granular gas: instantaneous plot of positions in 2D, in the inelastic regime. $N = 5000$, $\tau_c = 0.5$, $\tau_b = 100$ and $r = 0.1$.

where $\hat{\mathbf{n}}$ is the unit vector along the direction joining the centres of the particles; r is called the normal restitution coefficient. These rules reduce the longitudinal component of the relative velocity for $0 \leqslant r < 1$, which in contrast is only inverted at $r = 1$.

This model has been studied in detail [9, 10] through simulations using direct simulation Monte Carlo (DSMC) [14] and molecular dynamics (MD) algorithms [15] as well. The first method treats collisions stochastically, assuming the hypothesis of molecular chaos between particles at a distance smaller than σ_B (a parameter which is chosen to be smaller than the mean free path). It can be regarded as a sort of spatially inhomogeneous Monte Carlo technique. The second method implements the dynamics of the model without any approximation, requiring, however, much more computational resource.

In the dynamics of the N particles defined by equations (1), (2) and (3), (4), the relevant parameters are: the coefficient of normal restitution r, which determines the degree of inelasticity, and the ratio τ_b/τ_c of the forcing characteristic time (bath) to the 'global' mean free time between consecutive collisions. On the basis of these two parameters, the dynamics of our model exhibits two fundamental regimes:

- A stationary 'collisionless' regime occurring when $\tau_b \ll \tau_c$. In this regime we expect that, after a transient time of order τ_b, the system reaches the stationary behaviour of independent Brownian particles characterized by homogeneous density, Maxwell velocity distributions and the absence of correlations.
- A stationary 'colliding' regime obtained when $\tau_b \geqslant \tau_c$. If the collisions are inelastic, this condition corresponds to the *cooling* limit, and for times larger than τ_b, the model evolves with anomalous statistical properties.

Numerical simulations show that the thermodynamic limit on this model is well defined; thus one of the problems affecting the Du *et al* system is solved. The dynamics in the colliding regime ($\tau_b \geqslant \tau_c$) and in the presence of inelasticity ($r < 1$) results in a stationary state with a temperature T_g always lower than T_b. The granular temperatures approaches T_b monotonically as $r \to 1$, so the elastic limit can be safely taken without energy catastrophe. The fact that (when $r < 1$ and $\tau_b \geqslant \tau_c$) $T_g < T_b$ is the principal indication that our model of granular gas is a genuine non-equilibrium system in a statistically stationary state. This state is characterized by an inhomogeneous spatial arrangement of grains (clustering) and non-Gaussian velocity distributions. Figure 1 displays a snapshot, from 2D simulations, of the particle positions in a strong clustering regime. The inelastic regime exhibits much stronger density fluctuations than

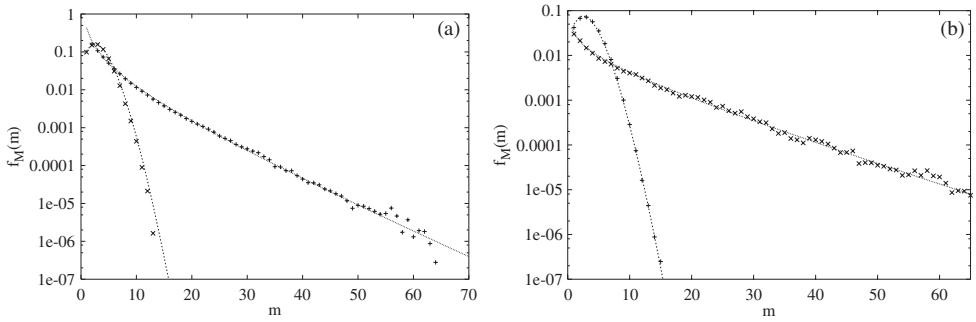

Figure 2. Density fluctuations in the homogeneously driven granular gas. Left: 1D case, with $N = 300$; the $\times$ are obtained in a collisionless regime, while the + correspond to a colliding regime with $r = 0.7$. Right: 2D case, with $N = 500$; the + are obtained in an almost elastic collisionless regime, the $\times$ corresponds to a colliding regime with $r = 0.5$. In both figures the collisionless case (equal to an elastic case) is fitted by a Poisson distribution, while the colliding inelastic case is fitted by an inverse power law with exponential cut-off, as discussed in the text.

those occurring in the collisionless limit, $\tau_b \ll \tau_c$, where grains, instead, occupy the whole volume uniformly with no correlations.

In figure 2, we show the probability distribution of the 'cluster mass', m, defined as the number of particles found in a box of volume V/M. We divided the container of the system into M identical boxes with an elementary volume V/M. In the collisionless regime, the number of particles in a box of size V/M follows a Poisson-like distribution with average $\langle m_M \rangle = N/M$. In contrast, the colliding regime ($\tau_b \gg \tau_c$) generates very different density distributions which can be fitted by a power law $m_M^{-\alpha_{cl}} \exp(-c_{cl} m_M)$ corrected by an exponential cut-off only due to finite size effects. In most of the simulations, we found $\alpha_{cl} > 1$ and $1/c_{cl}$ slightly greater than N/M. The power-law behaviour is the signature of self-similarity in the distribution of clusters occurring with no characteristic size. These anomalous density fluctuations are not an artefact produced by the simulation technique because they have been observed using both DSMC and MD algorithms. We have characterized the emergence of spatial correlations through the measure of the correlation dimension d_2 (Grassberger and Procaccia [16]). The latter is defined by the scaling behaviour $C(R) \sim R^{d_2}$ of the cumulated particle–particle correlation function

$$C(R) = \frac{1}{N(N-1)} \sum_{i \neq j} \overline{\Theta(R - |\mathbf{x}_i(t) - \mathbf{x}_j(t)|)} \sim R^{d_2} \tag{5}$$

where the over-bar indicates the time averaging taken after the system reaches a steady regime, R is the spatial resolution and $\Theta(u)$ is the unitary step function. For homogeneous density, d_2 coincides with the Euclidean dimension $d_2 = d$, while the result $d_2 < d$ is an indication of a *fractal* (self-similar) density. Model simulations carried out in the collisionless regime always lead to homogeneous distributions of particles (figure 3), while fractal densities often occur in inelastic colliding regimes ($\tau_b \gg \tau_c$). This is consistent with the scenario provided by the mass distribution of clusters discussed above. Another peculiarity of a driven granular gas is the behaviour of the velocity distribution $P(\mathbf{v})$. Typical $P(\mathbf{v})$ for our model in 1D and 2D simulations are shown in figure 4. We see a strong difference between the collisionless (or elastic) regime, $\tau_c \gg \tau_b$ and the inelastic colliding regime $\tau_c \ll \tau_b$. The collisionless regime is characterized by a Gaussian $P(\mathbf{v})$ while, in the colliding regime, a non-Gaussian behaviour appears as an enhancement of high-energy tails, and the fitting procedure of such tails provides the direct evaluation of the deviation from the Gaussian regime. In our simulations, we found evidence for $\exp(-v^{3/2})$ tails, in agreement with the theoretical prediction by Ernst and van

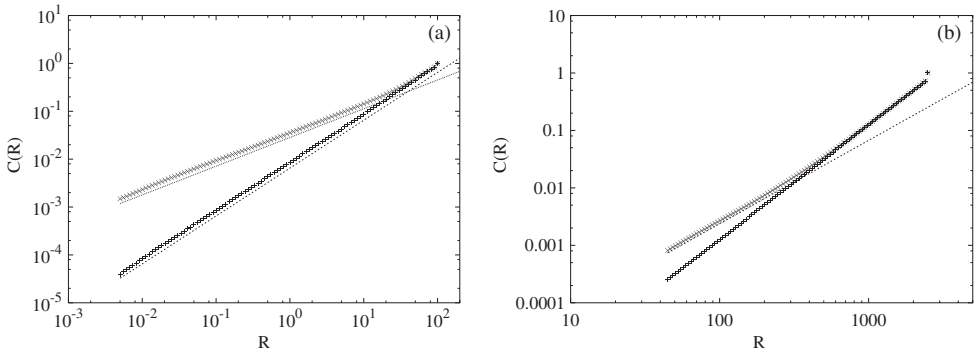

Figure 3. Density–density correlation function in the homogeneously driven granular gas. Left, in 1D ($N = 2000$) and right, in 2D ($N = 5000$). In both graphs the top (lower slope) curve corresponds to a colliding inelastic case, while the curve with the larger slope (corresponding to the exact dimensionality of the space) is obtained in a collisionless regime ($\tau_c \gg \tau_b$).

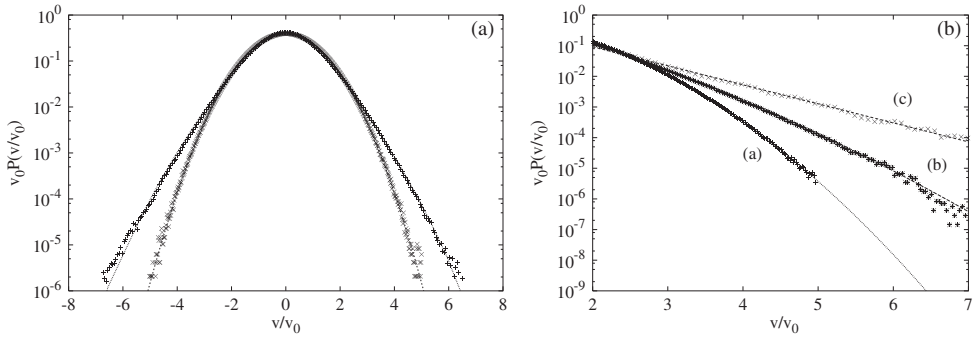

Figure 4. Velocity fluctuations in the homogeneously driven granular gas, in 1D (left) and 2D (right). The two situations in the left graph correspond to a collisionless regime (Gaussian fit) and colliding inelastic regime (non-Gaussian fit). The three situations in the right graph corresponds to: (a) a collisionless regime ($\tau \ll \tau_c$) with a distribution well fitted by a Gaussian; (b) an intermediate regime ($\tau_b \sim \tau_c$) with very low restitution coefficient ($r = 0.5$), fitted by an $\exp(-v^{3/2})$ curve; (c) a strongly colliding regime fitted by an exponential distribution.

Noije [17]. Remarkably, we see from the right panel of figure 4 that our model in the regime $\tau_c \ll \tau_c$ is also able to reproduce the exponential tails $\exp(-v)$ expected by the theory of [17] for 'homogeneous cooling states'. However, it is worth noticing that the result was derived with the assumption of spatial homogeneity, a condition violated by our simulations when the system undergoes clustering.

To our knowledge, experimental measurements of velocity distributions have been performed only recently and noticeably only for steady state granular systems under some sort of energy injection. We recall some of the laboratory set-ups used where non-Gaussian distribution have been observed:

(a) Vibration of the bottom of a 3D granular system [18].
(b) Vertical vibration of an horizontal plate with a granular monolayer on the top of it [19, 20].
(c) Vibration of the bottom side of an inclined plane with a very dilute granular monolayer rolling on it, under the presence of gravity [21].
(d) Vibration of the bottom of a granular system confined in a vertical plane [22].

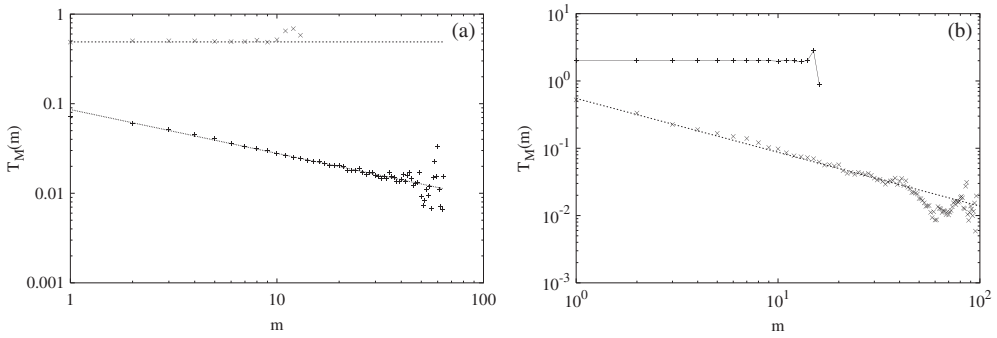

Figure 5. Temperature fluctuations in a homogeneously driven granular gas, in 1D (left) and 2D (right). In both figures the horizontal curves are obtained in a collisionless (or quasi-elastic) system, while the inverse power laws are observed in a colliding inelastic case.

One of the arguments given by Goldhirsch [23] to explain the existence of a general clustering instability starts from a heuristic estimate of the local temperature (granular temperature T_g) as a function of particle density n and local shear rate:

$$T_g \propto l_0^2 \propto n^{-2}, \tag{6}$$

where l_0 is the particle mean free path. The above relationship remains meaningful at timescales shorter than the decay time of the shear rate. Thus the local scalar pressure is supposed to decrease at larger densities $p = nT_g \propto n^{-1}$, implying an instability, because a positive fluctuation in the number of particles, in a given region, causes a reduction in the local pressure which attracts many other particles under the effect of pressure gradient. However, formula (6) strictly holds in the cooling regime and does not apply to our driven system for which the relation between local temperature T_g and local density is very different. Simulations, in fact, indicate that the mean square velocity $T_g(k)$, in the kth box, as a function of the number of grains m_k in that box, exhibits a more general power-law behaviour (the total volume has been divided in M identical boxes). As expected, in the clustering regime, the distribution of the number of particles in a box (cluster masses) presents a power-law decay with an exponential cut-off. This induces also a non-trivial power-law behaviour in the relation $T_g(k)$ versus m_k as reported in figure 5, where we see that in the collisionless (or elastic) regime the local temperature remains nearly constant, and so does not depend upon the cluster mass m. In the inelastic condition the local temperature appears to be a power of the cluster mass, $T_g(m) \sim m^{-\beta}$ with $0 < \beta < 1$. This relation ensures that the 'clustering catastrophe' (particles falling in an inverted pressure region) cannot occur because the scalar pressure $p = nT_g \propto n^{1-\beta}$ increases with the density since $1 - \beta$ is a positive exponent. Moreover, by using the previous result on the fractal correlation dimension d_2 (equation (5)), we can give an estimate of the length scale dependence of the temperature. In fact, if we assume that the scaling relation for the temperature is valid at different spatial scales, we can replace the *density* by the *number of particles* in the expression for T_g, i.e. $T_g(n) \sim n^{-\beta}$. Since the local density is expected to follow the scaling $n(R) \sim R^{-(d-d_2)}$, the local temperature follows the law $T_g(R) \sim R^{\beta(d-d_2)}$, and accordingly the local pressure behaves like $p(R) \sim R^{-(1-\beta)(d-d_2)}$. In conclusion, the density and the pressure both decrease with the length scale R, while the temperature increases. This scale dependence of the macroscopic fields is evidently at odds with the possibility of separating mesoscopic from microscopic scales and therefore the hydrodynamical description cannot be attempted. The inability of granular temperature to play the same role of kinetic temperature in equilibrium statistical physics (for example being equal to the temperature of the thermostat in the stationary

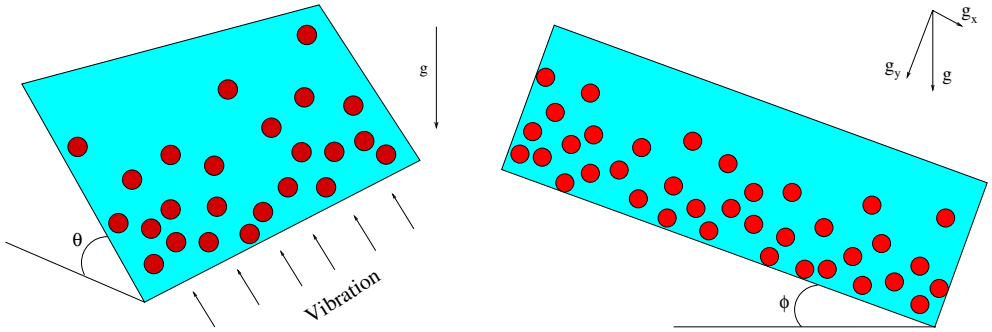

Figure 6. Left: sketch of the non-homogeneous model with gravity and vibrating bottom. Right: sketch of the non-homogeneous model with gravity and inclined bottom.

(This figure is in colour only in the electronic version)

asymptotic regime) is further demonstrated by models of granular mixtures [24]. Two granular materials, fluidized by the same kind of homogeneous random driving mechanism, show up different kinetic temperatures in agreement with experiments [25]. However, in the last section of this paper, we discuss a toy model where the granular temperature recovers a role similar to 'thermal temperature', making the situation even more complex.

3. Systems with a vibrating floor

Recent experiments [21] have investigated the effect of gravity on driven granular materials. Gravity, as a uniform force field, has no consequences on relative velocities and thus on the sequence of collisions. It simply accelerates the centre of mass of a granular gas and its action becomes relevant only when studied in the presence of particular boundary conditions that break the Galilean invariance (horizontal planes or plates). A plate has an important role in disordering the velocity distributions especially when it vibrates in the presence of gravity which, driving the grains toward the horizontal plates, makes the randomization process even much efficient.

The left frame of figure 6 sketches the geometry set-up of an experiment conducted in [21] consisting of a plane of size $L_x \times L_y$ inclined by an angle θ with respect to the horizontal. The top and the bottom wall confine particles to move in such a plane under the action of an effective gravitational force $g_e = g \sin\theta$. In our simulations, we reproduced the geometry and applied periodic boundary conditions in the horizontal direction. We assumed that both the top and the bottom walls of the plane are inelastic with a restitution coefficient r_w. The transfer of energy and momentum into the system is realized in our modelling through either sinusoidal or stochastic (thermal) vertical vibrations of the bottom wall. In the first case a particle bouncing onto this wall is reflected with a vertical velocity component: $v_y' = -r_w v_y + (1 + r_w)V_w$, where $V_w = A_w\omega_w \cos(\omega_w t)$ is the vibration velocity of the wall. In the second case, a particle, after the collision against the wall, acquires randomly new velocity components $v_x \in (-\infty, +\infty)$ and $v_y \in (0, +\infty)$ with probability distributions $P(v_y) = \frac{v_y}{T_w}\exp(-\frac{v_y^2}{2T_w})$ and $P(v_x) = \frac{1}{\sqrt{2\pi T_w}}\exp(-\frac{v_x^2}{2T_w})$, respectively, where $T_w = (A_w\omega_w)^2/2$ is the mean energy supplied by the wall to the gas in a period of oscillation.

For moderate vibration intensities, the model sets into an highly fluidized stationary phase which resembles turbulence. The time evolution of density and velocity fields exhibits

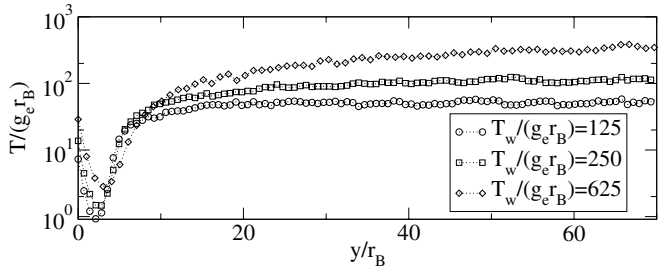

Figure 7. Temperature profiles versus the rescaled height y/r_{B} at three normalized forcing intensities $T_w/(g_e r_{\mathrm{B}})$, for the model with gravity and periodic vibrating bottom (figure 6)-left.

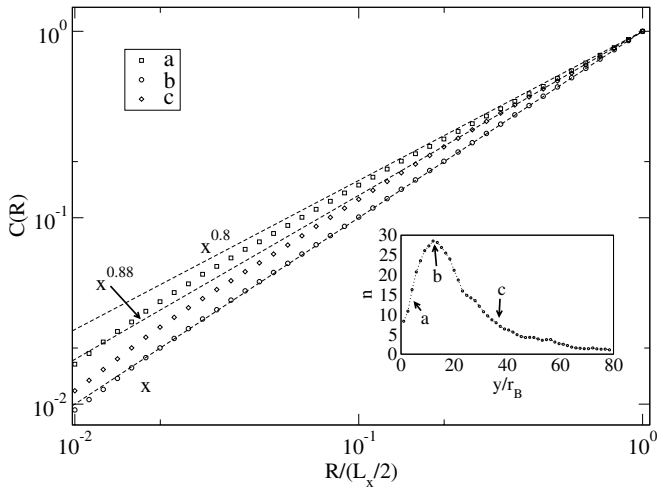

Figure 8. Function $C_{\Delta y}(y, R)$ for three stripes at different heights. The density profile as a function of the rescaled height is reported in the inset; labels a, b, c indicate the average densities and the heights of the slabs chosen to compute the three correlation curves in the main plot.

an intermittent-like behaviour characterized by rapid and large fluctuations, with sudden explosions (bubbles) followed by the formation of large particle clusters travelling coherently downwards under the action of gravity. In figure 7, we report the steady temperature profile $T_{\mathrm{g}}(y)$ for our system as obtained from simulations; a minimum of $T_{\mathrm{g}}(y)$ is clearly visible near $y = 0$, the position of the bottom wall. A parametric plot of the granular temperature T_{g} versus the particle density n determines a power law $T_{\mathrm{g}} \sim n^{-\beta}$ which closely recalls the algebraic tails already observed in the behaviour of the randomly driven model (section 2).

As before, the particle–particle correlation function is a useful indicator to quantify the degree of spatial arrangement in the system. In this case, a suitable quantity to measure is the particle–particle correlation function $C_{\Delta y}(y, R)$ conditioned to the height y, i.e. computed over the horizontal slab $B(y, \Delta y) = [y - \Delta y/2, y + \Delta y/2] \times [0, L_x]$. Data collected during simulations show a power-law behaviour $C_{\Delta y}(y, R) \sim R^{d_2(y)}$ (figure 8). Again, for homogeneous densities, d_2 is expected to coincide with the topological dimension of the box $B(y, \Delta y)$, so we obtained $d_2 = 1$ for all the resolutions $R \gg \Delta y$ at which the box appears as a 'unidimensional' stripe, while we found $d_2 = 2$, at resolutions $R \ll \Delta y$, because the slab appears as a two-dimensional object. When the regime of inelastic collisions is switched on, clustering processes, characterized by values of d_2 lower than the topological dimension, appear in some of the analysed stripes, as clearly seen by the three slopes of the log–log plot of figure 8. These three power laws refer to three slabs at different heights (labelled by a, b and c) and very different density conditions marked by the arrows in the inset showing the density profile. When the density is not too high, the fit performed in the region $R \gg \Delta y$ always yields an exponent smaller than 1.

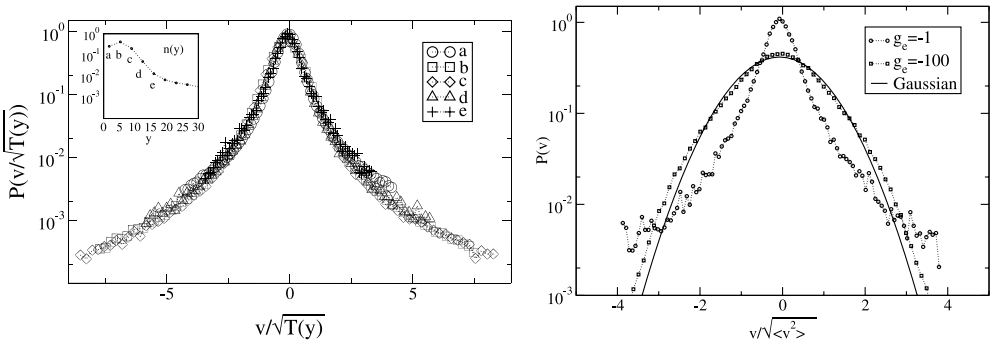

Figure 9. Left: collapse of horizontal velocity distributions in slabs a, b, c, d at different heights (see the inset), for the model with gravity and vibrating bottom. The log-linear plot highlights the non-Gaussian character of the tails. The inset displays the density profile as a function of the height from the bottom wall. Labels a, b, c, d indicate the corresponding heights of the stripes chosen to sample the velocity distributions. Right: horizontal velocity distributions for the same system with two different inclination of the plate, i.e. with two different values of the effective gravity g_e.

In the left frame of figure 9 we report the typical distributions of horizontal velocities for particles belonging to stripes at different levels (densities) above the bottom wall (a, b, c, d in the inset). The axis variables are properly rescaled to obtain a data collapse. Again, the distributions appear to be non-Gaussian, and their broadening, namely the granular temperature $T_g(y)$, is height dependent. The same behaviour can be observed for both periodic or stochastic vibrations. The right frame of figure 9 indicates that the distribution of horizontal velocities becomes more and more Gaussian when the angle of inclination is increased. This trend toward a Gaussian behaviour, in perfect agreement with experimental observations [21], is a consequence of a large inclination, which, enhancing the collision rate against the wall, favours the 'randomization' of velocities. According to the analogy between vibrating walls and heating baths, this scenario is consistent with that observed for the randomly driven model where larger 'heating rates' (decrease in τ_b/τ_c) determine a transition from a non-Gaussian to a Gaussian regime.

4. Acceleration onto an inclined plane

In the context of non-homogeneous driven granular gases, we analysed a second more interesting model [26], whose geometry is sketched in right frame of figure 6. The 'set-up' consists of a two-dimensional channel of depth L_y and length L_x, vertically confined by a bottom and a top inelastic wall; periodic boundary conditions are applied in the direction parallel to the flow. The channel is tilted up by an angle ϕ with respect to the horizontal line, so gravity has both components $g_x = g\sin\phi$ and $g_y = g\cos\phi$. This model mimics the experiment performed by Azanza *et al* [27], where a stationary flow in a two-dimensional inclined channel was observed at a point far from the source of the granular material. The assumption of periodic boundary conditions in the flow direction is consistent with the observed stationary regime reached upon the balance between gravity drift and damping effect due to inelastic collisions.

Simulated density, velocity and temperature profiles well reproduce those measured in experiments [27]. Indeed, they show the existence of a critical height, $H \sim 6\sigma_B$, corresponding to the separation between two different dynamical regimes. Below H, the profiles look almost linear, especially the density and velocity ones, while above H the profiles rapidly change

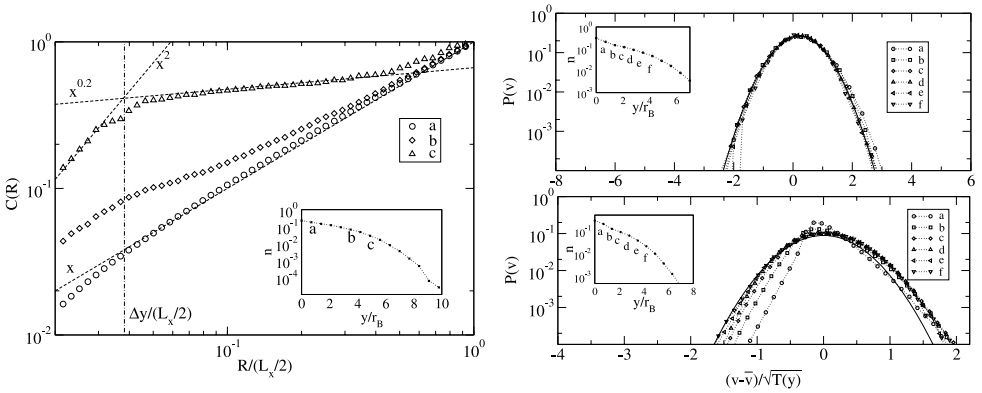

Figure 10. Left: density–density correlation function $C_{\Delta y}(y, R)$ in stripes a, b, c at different heights, as indicated in the inset, for the non-homogeneous model with an inclined bottom. The inset shows the density profile versus the rescaled height y/r_B and the letters a, b, c locate the heights y (or densities) of the stripes a, b, c chosen to compute $C_{\Delta y}(y, R)$. Right: horizontal velocities probability distribution function in stripes at different heights for the same model. The inset is as above.

and become nearly constant. These changes in the behaviour can be explained by the fact that, below H, transport is mainly dominated by collisional exchange, while above H it is mainly associated to ballistic flights. Again, our discussion focuses on the density correlations $C_{\Delta y}(y, R)$ computed in stripes at different densities (figure 10-left). Even in this system, clustering effects show up, and they are quantified by a correlation dimension d_2 ranging from 1 in homogeneous stripes to 0.2 for highly clustered stripes.

The distribution of horizontal velocities in slabs at different heights are plotted in the right frame of figure 10. The emergence of non-Gaussian behaviour is clearly evident, especially in the case with $r_w < r$ and mainly in the stripes near the bottom wall. The classical rheological model proposed by Jenkins and Richman [28] invokes a quasi-Gaussian equilibrium to calculate the transport coefficients. The results of our simulations, however, suggest that, near the bottom wall, the Gaussian approximation seems a very poor description of the real distribution. This is not only a consequence of inelasticity but also an effect of the proximity to the boundary, where high spatial gradients can easily bring the gas out of equilibrium. More recent derivations of hydrodynamic equations [29, 30] use a Boltzmann-like approach for inelastic gases which yields non-Gaussian velocity distributions: these theories pose a more solid basis and provide much more reliable estimations of transport coefficients.

5. The problem of scale separation

The reliability of hydrodynamics in the description of fluidized granular gases has been intensively probed through simulations and experiments suggesting, in some cases, a certain range of validity which surprisingly extends to very inelastic regimes. However, even in these lucky situations, the success is somehow lacking a rigorous foundation and addresses the question 'why does hydrodynamics work?'. Goldhirsch [23] for instance pointed out that 'the notion of a hydrodynamic, or macroscopic description of granular materials is based on unsafe grounds and it requires further study'. He argued that one of the main obstacles lies in the absence of a sharp distinction between the spatio-temporal scales of the microscopic dynamics and the relevant macroscopic scales. The aim of this section is to briefly review his arguments on this fundamental issue. We recall that the validity of hydrodynamics and its correct derivation is still a subject of debate, as recent discussions testify [32].

A standard granular experiment involves about 10^3–10^5 grains and a container with a linear size a few orders of magnitude larger than the typical size of grains. Therefore the possibility of identifying an intermediate scale separating microscopic kinetics from macroscopic hydrodynamics is rather doubtful. The lack of scale separation is not only a mere experimental limitation, because in principle one can imagine experiments involving an Avogadro's number of grains and very large containers. It is of conceptual nature and not only related to granular materials but also to molecular gases when subject to large shear rates or large thermal gradients. In general, when the velocity or the temperature fields vary significantly over a length of a mean free path, no scale distinction occurs between microscopic and macroscopic scales; accordingly, the gas should be considered mesoscopic. In granular gases, this kind of *mesoscopicity* is generic and not limited to the presence of strong forcing. Moreover, phenomena like clustering, collapse and avalanches typical of granular dynamics strongly violate the *molecular chaos* condition required by the Boltzmann approach. In mesoscopic systems, fluctuations are expected to be larger, and by consequence the ensemble averages of observables need not be representative of their typical values. Furthermore, in systems without a true scale separation, like turbulent fluids or systems undergoing a second-order phase transition, one expects that the constitutive relations relating fluxes to densities are scale dependent.

The quantitative demonstration of the intrinsic mesoscopic nature of granular gases stems from the equation $T_g \propto \gamma^2 l_0^2/(1-r^2)$ [31], relating the local granular temperature T_g to the local shear rate γ and to the mean free path l_0. The above relation holds until γ can be considered a slow varying (decaying) quantity with respect to much more rapid damping rates of the temperature fluctuations. Then, the ratio between the variation of the macroscopic velocity $\delta v \sim \gamma l_0$ due to the shear and the thermal speed $v_T = \sqrt{T}$ is proportional to $\sqrt{1-r^2}$. Apart from very low values of $1-r^2$, the shear rate is always large, and thus the Chapman–Enskog expansion leading to the hydrodynamic theory for the system should be generally carried out beyond the Navier–Stokes order. The above consideration is a direct consequence of the supersonic nature of granular gases [23]. It is clear that a collision between two particles moving in the same direction reduces their relative velocity but not the sum of their momenta. In a number of such collisions, the velocity fluctuations may become very small with respect to $\delta v \sim \gamma l_0$. We have to say that even the notion of mean free path may become useless in a shear experiment because the mean square particle velocity is given by $\gamma^2 y^2 + T$ (y being the direction of the shear). When $y \gg \sqrt{T}/\gamma$, the distance covered by a particle in the mean free time τ is $l(y) = y l_0 \gamma/\sqrt{T} = y\sqrt{1-r^2}$, which may become much larger than the 'equilibrium' mean free path l_0 and even greater than the system size in the streamwise direction. The ratio between the mean free time $\tau = l_0/\sqrt{T}$ and the macroscopic characteristic time of the problem $1/\gamma$ is again proportional to $\sqrt{1-r^2}$. Therefore a sharp separation between microscopic and macroscopic timescales rigorously occurs only when $r \to 1$ independently of system and grain sizes. Two serious problems thus arise: (a) the fast local equilibration allowing for the use of equilibrium distributions as zeroth-order approximations is not obvious; (b) the stability studies based on the linearization of hydrodynamic equations become meaningless, since they predict instabilities on timescales which hydrodynamics is not supposed to resolve.

Goldhirsch [23] has also shown that the absence of a neat distinction in space/timescales implies a scale dependence of fields and fluxes; in particular, the pressure tensor depends on the coarse graining resolution used to take local averages. This is similar to what happens, for example, in turbulence, where the 'eddy viscosity' is scale dependent. Pursuing this analogy, Goldhirsch has noted that an intermittent behaviour can be observed in the time series of experimental and numerical measures of the pressure tensor. Single collisions, which are

usually averaged out in molecular systems, appear in granular systems as 'intermittent events' affecting the time behaviour of relevant observables.

6. Granular temperature in a simple double-well model

So far, through the review of some models of inelastic gases, we have given evidence for the non-thermodynamics nature of the parameter T_g called 'granular temperature'. We have indeed shown that T_g is usually different from the thermostat temperature; it can be very inhomogeneous even in homogeneously driven systems and may strongly depend upon the scale of observation. Finally, we have mentioned the fact that, in granular mixtures, T_g does not govern the energy balance. In this section we want to show that T_g still maintains the role of parameter controlling the characteristic times of the granular dynamics. Here we discuss a simple toy model in which the main ingredient of granular gases, the inelasticity, is at work, but the dynamics is characterized by a timescale determined by the granular temperature through an Arrhenius-like formula [33].

The model consists of two inelastic hard rods (the simplest granular gas) constrained to move on a line under the effect of a bistable external potential $U(x) = -ax^2/2 + bx^4/4$. The system is coupled to a bath which exerts upon particles a velocity-dependent friction and a random force. In the absence of collisions, the particles evolve according to

$$M\frac{\mathrm{d}^2 x_i}{\mathrm{d}t^2} = -M\gamma\frac{\mathrm{d}x_i}{\mathrm{d}t} - U'(x_i) + \xi_i(t) \tag{7}$$

where the prime indicates the spatial derivative, x_i ($i = 1, 2$) represents the position of particles, γ is a friction coefficient and $\xi_i(t)$ is the stochastic driving force with variance $\propto T_b$.

The basic phenomenology of the model is illustrated in figure 11. The relative particle distance, $y = x_2 - x_1$, fluctuates in time showing time intervals of average lifetime τ_2, when particles are confined to the same well ($y \sim d$) alternated with intervals, of average lifetime τ_1, when particles sojourn in separate wells. The dynamics is dominated by two competing effects, the dissipation in the collisions and the excluded volume. The first brings the particles together in the same well (clustering) while the other favours their staying apart in different wells. These two opposite effects are responsible for the existence of τ_1 and τ_2 as different timescales. Figure 12 shows that τ_2 and τ_1 follow an Arrhenius behaviour with a suitable parameter renormalization with respect to the independent particle problem:

$$\tau_k \approx \exp\left[\frac{W_k}{T_k}\right], \tag{8}$$

where $k = (1, 2)$ indicates single or double occupation of a well, $W_1 = \Delta U$ (ΔU being the energy barrier between the wells) and $W_2 = \Delta U - \delta U < \Delta U$. The correction δU to the energy barrier ΔU amounts to $a(d/2)^2 + b/4(d/2)^4$ and takes into account the effect of the excluded volume repulsion. When two grains belong to the same well their centre of mass lies higher than if they were in separate wells, therefore each grain experiences a lower (effective) energy barrier. This is a typical correlation effect, because the repulsion makes the double occupancy of a well less likely, with respect to the non-interacting case. The smaller the ratio of the well width to the particle diameter, the stronger the reduction of the escape time [34, 35]. In figure 12 and the related inset, the reader can see that the plots of τ_1 and τ_2 of the inelastic system (dark symbols) intersect at a certain temperature $T_b = T_c$. Below T_c the time τ_2 becomes smaller than τ_1. The origin of this crossover lies in the fact that, in the inelastic system, temperatures T_2 and T_1 are no longer equal to T_b, and furthermore $T_2 < T_1$. Thus, the mean lifetime of the clustering regimes can still be described by expression (8), but

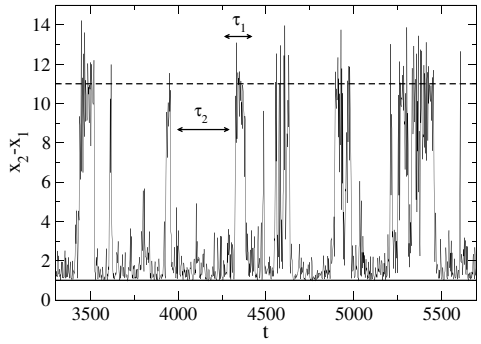

Figure 11. Relative distance $x_2 - x_1$ as a function of time for a system with $r = 0.9$ and $T_b = 4.0$. The solid line indicates the diameter of the rods $d = 0.1$, while the dashed line marks the well separation $L \simeq 10.95$ (for potential parameters $a = 0.5$ and $b = 0.01$).

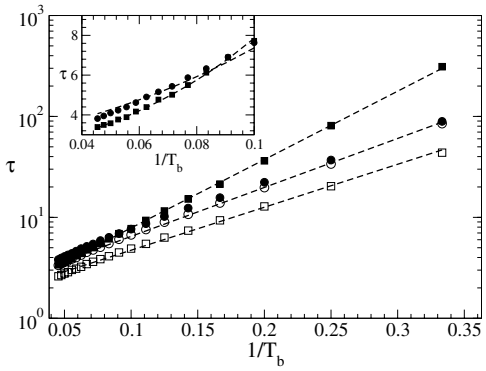

Figure 12. Arrhenius plot of mean escape times τ. Open symbols refer to the elastic case: the escape time is τ_1 (circles) when a well is singly occupied, τ_2 (squares) when a well is doubly occupied. Full symbols correspond to the inelastic system ($r = 0.9$). Linear behaviour indicates the validity of Kramer's theory with renormalized parameters, and the slopes agree with values obtained from equation (8). Inset: enlargement of the crossover region where τ_2 becomes smaller than τ_2. The arguments of the exponentials (dashed lines) in the same figure have been obtained by formula (8).

now the granular effect competes with the excluded volume correction, eventually leading to $\tau_1 > \tau_2$.

A simple argument can be used to estimate the shift of T_2 from T_b. For moderate driving intensity, T_1 is nearly equal to T_b, while T_2 is lower than T_b by a factor which depends on the inelasticity. Simulations show that T_2 varies linearly with T_b and its slope is a decreasing function of the inelasticity $(1 - r)$. A good estimate of temperature T_2 can be obtained by an energy balance argument when the two particles belong to the same well regarded as an harmonic well $V(x) = \omega_{\min}^2 x^2/2$. The average power per particle satisfies the balance equation

$$\overline{\frac{dE}{dt}} = 2\gamma(T_b - T_2) + \overline{\frac{\delta E_c}{2\tau_c}} \tag{9}$$

where $2\gamma(T_b - T_2)$ stems from the competition between the viscous damping $(-2\gamma T_2)$ and the power supplied by the stochastic driving $(2\gamma T_b)$, while the last term on the right-hand side of equation (9) estimates the mean power dissipated in each collision, τ_c being the typical collision time. From the rule (3) applied in 1D, we have $\delta E_c = -(1 - r^2)(v_2 - v_1)^2/4$. At stationarity, we expect that $\overline{dE/dt} \sim 0$, thus

$$T_2 = T_b - \frac{1 - r^2}{8\gamma\tau_c}\overline{(v_2 - v_1)^2}.$$

Assuming that the precollisional velocities v_1 and v_2 are nearly independent, we can approximate $\overline{(v_2 - v_1)^2} \simeq \langle v_1^2 \rangle + \langle v_2^2 \rangle = 2T_2$.

The collision time τ_c is estimated through the oscillation frequency in the harmonic well $\tau_c = \pi/\omega_{\min}$, where the factor $1/2$ stems from the excluded volume effect. Finally, we write the formula

$$T_2 = \frac{T_b}{1 + q(1 - r^2)} \tag{10}$$

for the granular temperature, with $q = \omega_{\min}/(4\pi\gamma)$. The knowledge of T_2 and ΔU characterizes the jump dynamics of the system across the energy barrier even when it is inelastic. Numerical simulations of equations (7) verify the relation (10) very well.

This simple example demonstrates that the granular temperature, even if cannot control the 'equilibrium' behaviour of a granular gas, fairly determines the typical dynamical timescales of the system.

7. Conclusions

We have summarized the main lines of research carried out during recent years on granular gases. This paper focuses on the theoretical basis of a fluid-like description of granular systems under strong external forcing. In experiments, the behaviour of a granular gas strongly resembles that of a fluid. However, it is never at thermal equilibrium and, even though a kinetic temperature can be defined and measured, it has not the same role of equilibrium temperature. Moreover, many conceptual concerns, such as the absence of space and timescale separation, suggest that the hydrodynamics is well posed only in a limited range of parameters. We have introduced a family of models of granular gases under external forcing to investigate these issues. Such models, addressing different physical situations, present common features: strong correlated density fluctuations (clustering), non-Gaussian behaviour of velocity distributions with heavy tails, and lack of energy equipartition or thermalization. The first model, an inelastic gas under external stochastic driving, is of course the simplest and most idealized, but it displays all these features straightforwardly, demonstrating that the main ingredient leading to such anomalous behaviour is simply the inelasticity.

However, the situation is not so hopeless: kinetic theories (used to build hydrodynamics) work in the neighbourhood of the elastic limit, when all the above problems appear in a mild form. More surprisingly, there are cases where some predictions of usual statistical mechanics and thermodynamics are also reliable in strong inelastic conditions. We considered, as an example, the dynamics of a couple of granular particles in a double well potential, which again can be characterized by an Arrhenius behaviour provided that the environment temperature is replaced by the granular temperature. Furthermore, some of us [36, 37] have also shown that Green–Kubo relations for the response to linear perturbation are still valid, again substituting granular temperature for external bath temperature (there have been several attempts to derive Green–Kubo relations for granular gases; see for example [38]). Both these results are quite intriguing because they appear to be valid in strongly out-of-equilibrium regimes.

References

[1] Jaeger H M, Nagel S R and Behringer R P 1996 *Rev. Mod. Phys.* **68** 1259 and references therein

[2] Pöschel T and Luding S (ed) 2001 *Granular Gases* (*Springer Lecture Notes in Physics* vol 564) (Berlin: Springer)

[3] Pöschel T and Brilliantov N V (ed) 2003 *Granular Gas Dynamics* (*Springer Lecture Notes in Physics* vol 624) (Berlin: Springer)

[4] Du Y, Li H and Kadanoff L P 1995 Breakdown of hydrodynamics in a one-dimensional system of inelastic particles *Phys. Rev. Lett.* **74** 1268

[5] Sela N and Goldhirsch I 1995 Hydrodynamics of a one-dimensional granular medium *Phys. Fluids* **7** 507

[6] Kadanoff L P 1999 Built upon sand: theoretical ideas inspired by granular flows *Rev. Mod. Phys.* **71** 435

[7] Jaeger H M, Knight J B, Liu C-h and Nagel S R 1994 What is shaking in the sandbox? *Mater. Res. Bull.* (May) 25

[8] Knight J B, Fandrich C G, Lau C N, Jaeger H M and Nagel S R 1995 Density relaxation in a vibrated granular material *Phys. Rev.* E **51** 3957

[9] Puglisi A, Loreto V, Marini-Bettolo-Marconi U, Petri A and Vulpiani A 1998 Clustering and non-Gaussian behavior in granular matter *Phys. Rev. Lett.* **81** 3848

[10] Puglisi A, Loreto V, Marini-Bettolo-Marconi U and Vulpiani A 1999 A kinetic approach to granular gases *Phys. Rev.* E **59** 5582

[11] Williams D R M and MacKintosh F C 1996 Driven granular media in one dimension: correlations and equations of state *Phys. Rev.* E **54** R9–12
[12] van Noije T P C, Ernst M H, Trizac E and Pagonabarraga I 1999 Randomly driven granular fluids: large scale structures *Phys. Rev.* E **59** 4326
[13] Kubo R, Toda M and Hashitune N 1978 *Statistical Physics II: Nonequilibrium Statistical Mechanics* (Berlin: Springer)
[14] Bird G A 1994 *Molecular Gas Dynamics and the Direct Simulation of Gas Flows* (Oxford: Clarendon)
[15] Cecconi F, Diotallevi F, Marini-Bettolo-Marconi U and Puglisi A 2004 Fluid-like behavior of a one-dimensional granular gas *J. Chem. Phys.* **120** 35
[16] Grassberger P and Procaccia I 1983 Characterization of strange attractors *Phys. Rev. Lett.* **50** 346
[17] van Noije T P C and Ernst M H 1998 Velocity distributions in homogeneously cooling and heated granular fluids *Granular Matter* **1** 57
[18] Losert W, Cooper D G W, Delour J, Kudrolli A and Gollub J P 1999 Velocity statistics in excited granular media *Chaos* **9** 682
[19] Olafsen J S and Urbach J S 1998 Clustering, order and collapse in a driven granular mono-layer *Phys. Rev. Lett.* **81** 4369
[20] Olafsen J S and Urbach J S 1999 Velocity distributions and density fluctuations in a 2D granular gas *Phys. Rev.* E **60** R2468
[21] Kudrolli A and Henry J 2000 Non-Gaussian velocity distributions in excited granular matter in the absence of clustering *Phys. Rev.* E **62** R1489
[22] Rouyer F and Menon N 2000 Velocity fluctuations in a homogeneous 2D granular gas in steady state *Phys. Rev. Lett.* **85** 3676
[23] Goldhirsch I 1999 Scales and kinetics of granular flows *Chaos* **9** 659
[24] Garzó V and Dufty J 1999 *Phys. Rev.* E **60** 5706
Marini-Bettolo-Marconi U and Puglisi A 2002 *Phys. Rev.* E **65** 051305
Marini-Bettolo-Marconi U and Puglisi A 2002 *Phys. Rev.* E **66** 011301
Pagnani R, Marini-Bettolo-Marconi U and Puglisi A 2002 *Phys. Rev.* E **66** 051304
Barrat A and Trizac E 2002 *Granular Matter* **4** 57
[25] Feitosa K and Menon N 2002 *Phys. Rev. Lett.* **88** 198301
Wildman R D and Parker D J 2002 *Phys. Rev. Lett.* **88** 064301
[26] Baldassarri A, Marini-Bettolo-Marconi U, Puglisi A and Vulpiani A 2001 Granular gases under gravity *Phys. Rev.* E **64** 011601
[27] Azanza E, Chevoir F and Moucheront P 1997 Experimental study of rapid granular flows in a two-dimensional channel *Powder & Grains* vol 97, ed R P Behringer and J T Jenkins (Rotterdam: Balkema) p 455
[28] Jenkins J T and Savage S B 1983 A theory for the rapid flow of identical, smooth, nearly elastic, spherical particles *J. Fluid Mech.* **130** 187
[29] Sela N and Goldhirsch I 1998 Hydrodynamics equations for rapid flows of smooth inelastic spheres, to Burnett order *J. Fluid Mech.* **361** 41
[30] Brey J J, Dufty J W, Kim C S and Santos A 1998 *Phys. Rev.* E **58** 4638
Brey J J, Ruiz-Montero M J and Moreno F 2000 *Phys. Rev.* E **62** 5339
Brey J J, Ruiz-Montero M J and Moreno F 2001 *Phys. Rev.* E **63** 061305
[31] Goldhirsch I and Zanetti G 1993 Clustering instability in dissipative gases *Phys. Rev. Lett.* **70** 1619
[32] Dufty J W and Brey J J 1999 *Phys. Rev. Lett.* **82** 4566
Tan M-L and Goldhirsch I 1999 *Phys. Rev. Lett.* **82** 4567
[33] Cecconi F, Puglisi A, Marini-Bettolo-Marconi U and Vulpiani A 2003 Noise activated granular dynamics *Phys. Rev. Lett.* **90** 064301
[34] Marini-Bettolo-Marconi U and Tarazona P 1999 Dynamic density functional theory of fluids *J. Chem. Phys.* **110** 8032
[35] Cecconi F, Marini-Bettolo-Marconi U, Puglisi A and Diotallevi F 2004 Inelastic hard-rods in a periodic potential *J. Chem. Phys.* **121** 5125
[36] Puglisi A, Baldassarri A and Loreto V 2002 Fluctuation–dissipation relations in driven granular gases *Phys. Rev.* E **66** 061305
[37] Barrat A, Loreto V and Puglisi A 2004 Temperature probes in binary granular gases *Physica* A **334** 513
[38] Brilliantov N and Pöschel T 2000 *Phys. Rev.* E **61** 1716
Goldhirsch I and van Noije T P C 2000 *Phys. Rev.* E **61** 3241
Brey J J, Dufty J W and Ruiz-Montero M M 2003 *Granular Gas Dynamics* ed T Pöschel and N Brilliantov (New York: Springer) p 227 and references therein
Garzó V 2004 *Physica* A **343** 105